

A case study in the local estimation of shear-wave logs

Brian H. Russell, Laurence R. Lines and Daniel P. Hampson

ABSTRACT

In this case study, we utilize the techniques of multi-linear regression and cross-validation to develop a relationship between shear-wave logs and a suite of other well log curves. This relationship is then used to predict pseudo shear-wave log curves in wells that do not contain shear-wave information. The relationship that is derived in this study can be seen as an improvement on the standard linear relationship used to predict shear-wave logs (Castagna et al., 1985). However, it is important to note that the relationship derived here is strictly valid only within the area of study. We therefore feel that this work presents an approach to building local relationships within specific areas of study, rather than presenting a universal equation that can be used everywhere.

INTRODUCTION

In this case study, we will be using nine wells within the survey area of a 3C-3D seismic dataset acquired over the Blackfoot region of Alberta (Dufour et al., 2002). In this paper, we will not be using the seismic data. The well log input consists of nine wells, each with P-wave sonic, density, and gamma ray, and three with S-wave sonic. Figure 1 shows the distribution of wells throughout the 3D survey area, and the three wells that contain S-wave logs have been indicated with arrows. The map has been rotated so that north is pointing to the right.

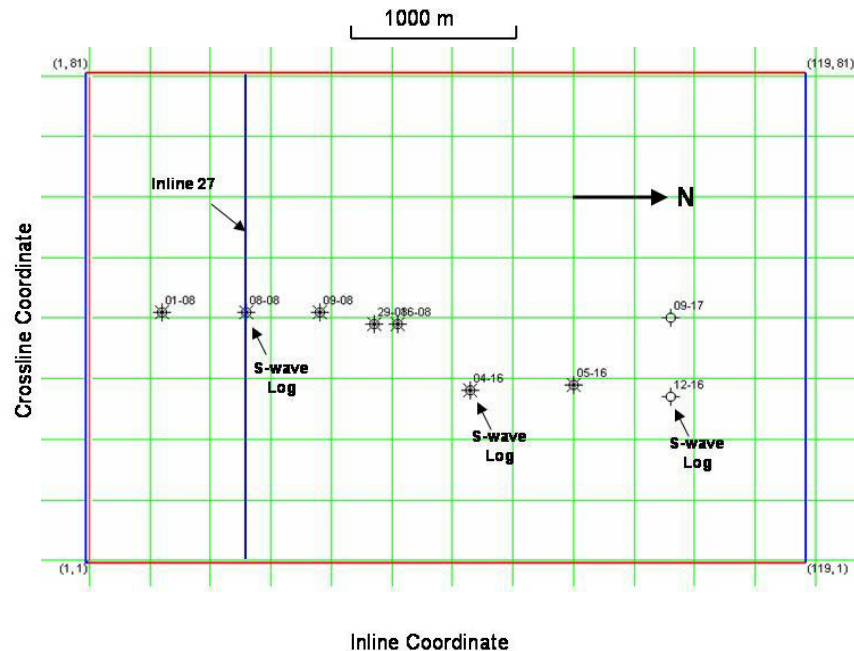


FIG. 1. A map of the wells used in this study, with wells with shear-wave logs indicated.

The objective of this study is to derive a relationship between the S-wave log and the P-wave sonic, density, and gamma ray logs in the wells in which all are present. We will then apply this relationship to the wells in which the S-wave log is not present, and create pseudo-S-wave logs.

S-WAVE LOG STATISTICAL ANALYSIS

The traditional approach to S-wave curve prediction (Castagna et al., 1985) is to find the linear regression fit between the P-wave and S-wave curves given by the regression equation

$$V_s = a + bV_p . \tag{1}$$

Although it is preferable to derive the regression coefficients a and b from local wells, a reasonable fit can usually be found using the coefficients given by Castagna et al. (1985). In this study, we will not assume a pre-existing relationship as in Equation 1, but will rather determine a multi-linear regression relationship using the available data. The logs from one of the three wells in which the S-wave sonic log is present, well 04-16, are shown in Figure 2.

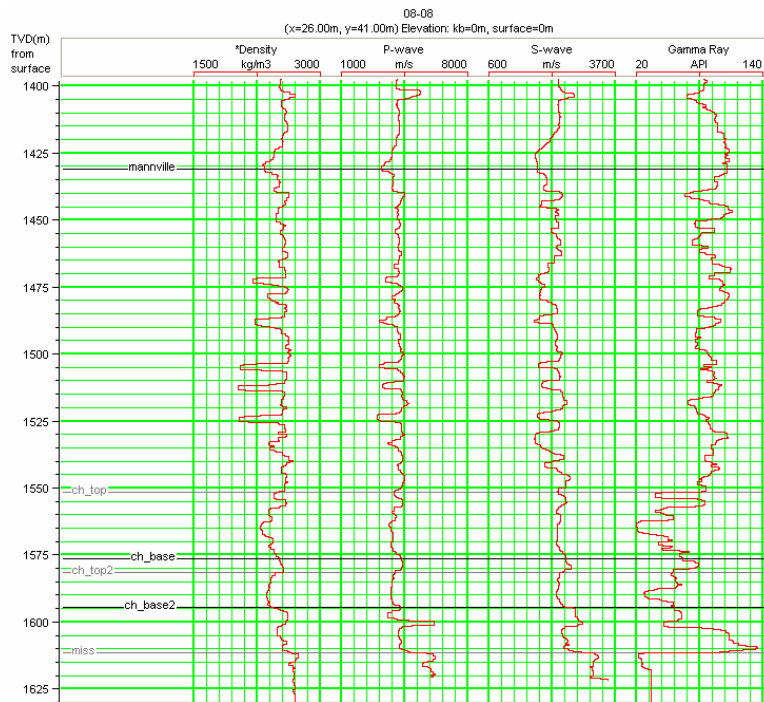
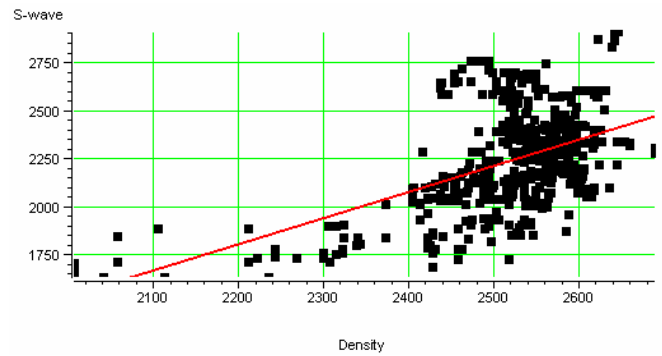
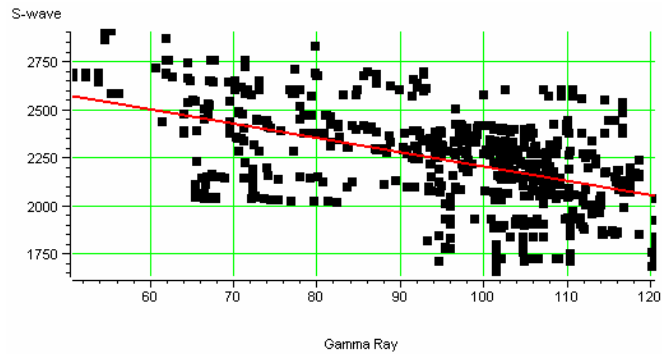


FIG. 2. The well log curves for well 04-16 in Figure 1.

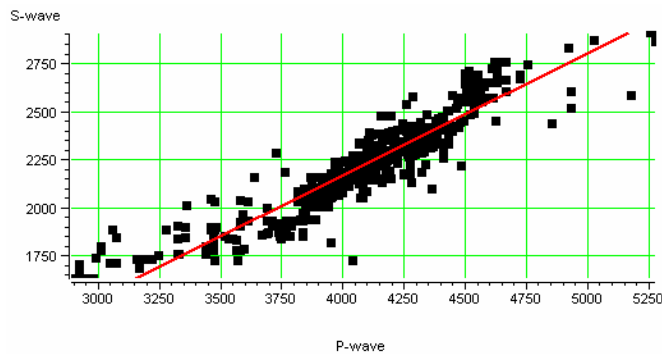
In Figure 2, it would appear that the S-wave curve and the P-wave curve match each other the closest. However, there is also a reasonable match between the S-wave curve and both the gamma ray and density curves. To quantify this observation, Figure 3 shows the correlations between S-wave log and the density log, gamma ray log, and the P-wave log, respectively, for well 04-16.



(a)



(b)



(c)

FIG. 3. The crossplots of S-wave velocity against (a) density, (b) gamma ray and (c) P-wave velocity for the curves in well 04-16 from Figure 2.

For each of the three regressions shown in Figure 3, we can write the generalized form of Equation 1 as

$$V_s = a + bL, \quad (2)$$

where L represents either the density, gamma ray or P-wave sonic log. The regression coefficients, correlation coefficients and errors given for the plots of Figure 3 are shown in Table 1. In this table, we see that the P-wave fit is the best, as expected, and that the

density fit is slightly better than the gamma ray fit. Notice that the gamma ray curve has a negative correlation with the S-wave curve.

Table 1. The statistics for the crossplots from well 04-16, shown in Figure 3.

S-wave vs:	P-wave	Density	Gamma
Intercept(<i>a</i>)	-366.95	-1182.76	2948.41
Slope (<i>b</i>)	0.634	1.357	-7.434
Corr. Coeff.	0.9305	0.5030	-0.4845
RMS Error	92.251	217.683	220.329

For the other two wells, not shown here, the fits are different. For well 08-08, the P-wave, density and gamma ray correlation coefficients are 0.777, 0.538, and -0.246, respectively. For well 12-16, the correlation coefficients are 0.490, 0.328, and -0.386, indicating that in this well the P-wave fit is quite poor and the gamma ray fit is slightly better than the density fit.

The result of combining all three wells is shown in Table 2, arranged in order of increasing RMS error and decreasing correlation coefficient. As expected, the P-wave log correlates best, followed by the density log, followed by the gamma ray log.

Table 2. The statistics for all three of the wells with S-wave logs shown in Figure 1.

Target	Attribute	Error	Correlation
S-wave	P-wave	165.154755	0.730677
S-wave	Density	218.033646	0.433163
S-wave	Gamma Ray	226.306885	-0.353285

MULTILINEAR REGRESSION FOR LOG PREDICTION

We next applied the linear regression technique to build relationships between the S-wave log and the other logs. We first considered the regression of S-wave against P-wave velocity. Using Equations 1 and 2, the regression coefficients were computed using the P-wave and S-wave values for all three wells. These coefficients were computed to be

$$V_s = 269.125 + 0.480V_p. \tag{3}$$

We will next find the coefficients using a multilinear approach, and including all possible well curves. The multilinear regression equation is given by

$$V_s = a + bV_p + c\rho + d\gamma, \tag{4}$$

where ρ is the density log and γ is the gamma ray log.

The log attributes and coefficients in Equation 4 were determined using a technique in which cross-validation is used to determine the optimal ordering of attributes (Hampson et al., 2001). The results of performing the linear multi-attribute analysis are shown in Figure 4, where the bottom curve (black) shows the total training error and the top curve (red) shows the validation error.

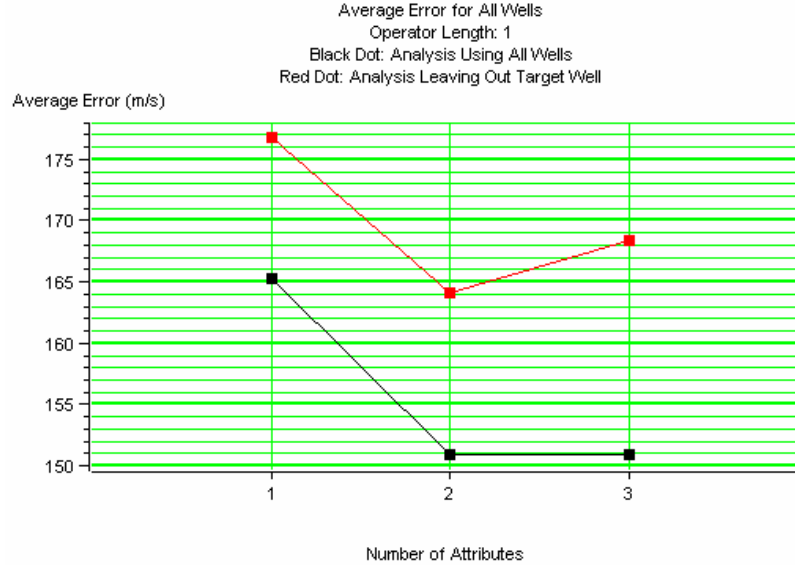


FIG. 4. Training results for the multilinear regression, where the bottom curve shows the total training error and the top curve (red) shows the cross-validation error.

In Figure 4, the training error is the error using all three wells in the prediction, and the cross-validation error is the error in which the well to be predicted is left out of the training. Two results are clear from this plot. First, when the multilinear regression technique is used, the gamma ray log is the second best log attribute to use. This was not clear when the regression was applied to each log attribute independently. Second, the validation error shows that the error increases when the density log is added, indicating that the optimum fit is found by using only the P-wave and gamma ray logs in the multilinear regression. The regression coefficients in this analysis were found to be

$$V_s = 656.47 + 0.461V_p - 3.505\gamma. \quad (5)$$

In Equation 5, note that the gamma ray has a negative coefficient. This is due to the negative correlation of the gamma ray log with the S-wave log, as seen in Tables 1 and 2. A better fit can be introduced by applying nonlinear functions, such as the inverse, log, square and square root, to the attributes before performing the regression fit. The optimum nonlinear functions found using cross-validation were the square root of gamma ray and the inverse of density. However, the density log again increased the cross-validation error and was therefore dropped from the result. The regression coefficients in this analysis were found to be

$$V_s = 893.42 + 0.465V_p - 60.46\sqrt{\gamma}. \quad (6)$$

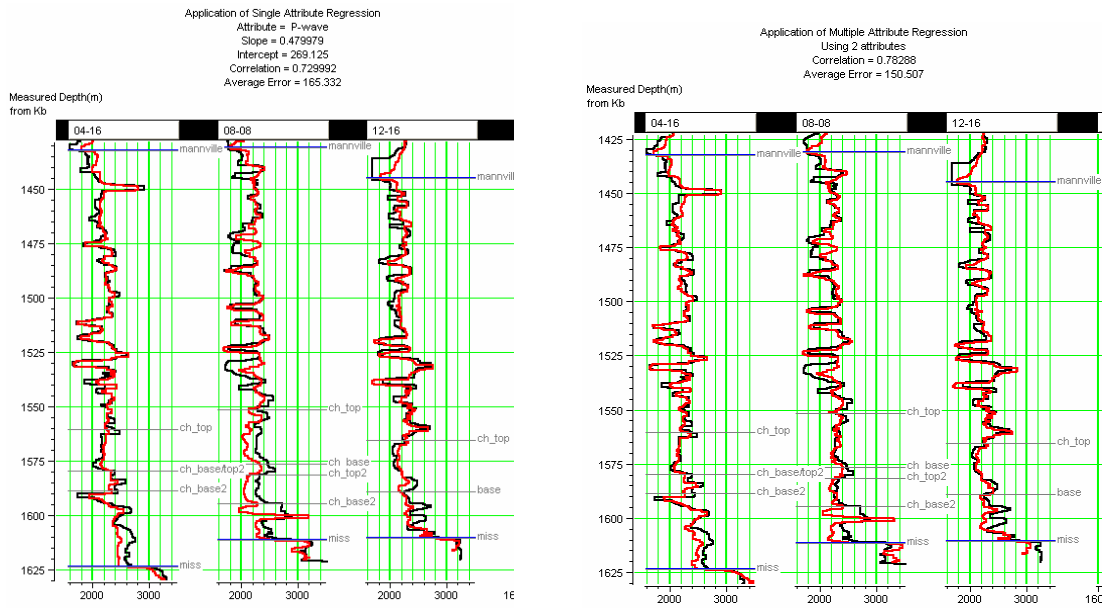


FIG. 5. Figure (a) shows the training results for regression with the P-wave sonic log alone and figure (b) shows regression with P-wave and gamma ray logs.

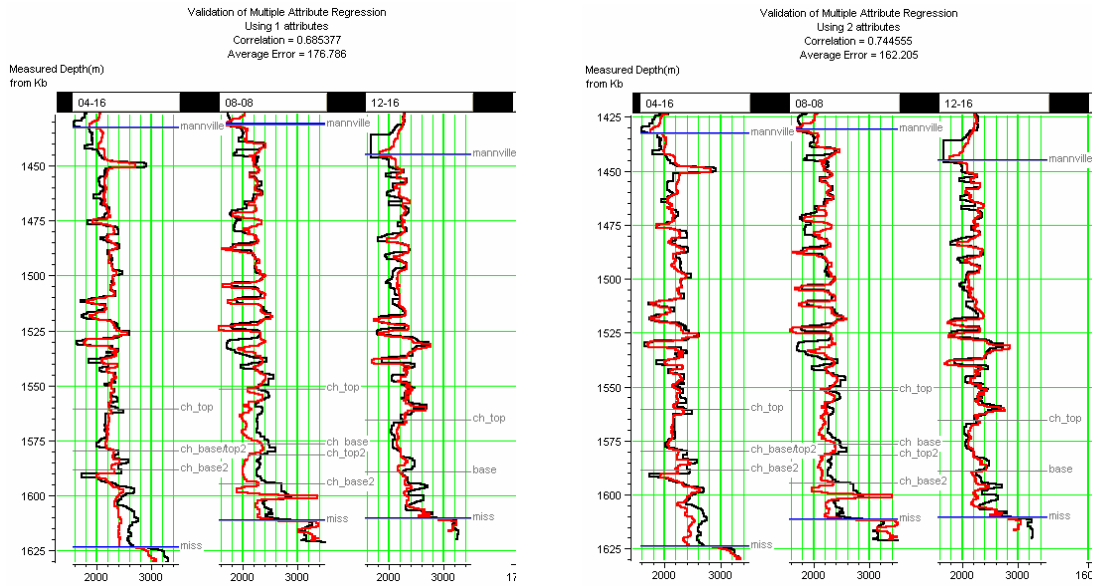


FIG. 6. Figure (a) shows the validation results for regression with the P-wave sonic log alone and figure (b) shows regression with P-wave and gamma ray logs.

This relationship suggests that the shear wave velocity is sensitive to the clay content of the formation being measured. The resulting pseudo-sonic logs are shown in Figures 5 and 6, where Figure 5 shows the training results, in which all the wells were used in the prediction, and Figure 6 shows the validation result, in which the application well is left out of the training. In both Figures 5 and 6, regression on P-wave alone is shown in Figures 5a and 6a, and multilinear regression with both P-wave and gamma ray logs is shown in Figures 5b and 6b.

In Figure 5 it is obvious that the addition of the gamma ray log has improved the fit. The improvement is quite small in well 04-16, where the correlation between S-wave and P-wave values was very high (Table 1), but is noticeable in the deeper section of well 08-08. Also, notice that the correlation coefficient has gone from 0.73, in the single regression case, to 0.78, in the multiple regression case.

Figure 6, which shows the validation results, also shows improvement between the single regression case and the multiple regression case. As expected, the correlation coefficients are smaller than for the training case, and the correlation coefficient has now improved from 0.68, in the single regression case, to 0.74 in the multiple regression case.

CONCLUSIONS

In this case study, we developed a relationship between shear-wave logs and a suite of other well log curves, and then used this relationship to predict pseudo shear-wave log curves in wells that did not contain shear-wave information. Although the relationship that was derived in this study was shown to be an improvement on the standard linear relationship used to predict shear-wave logs, it is felt that this work presents an approach to building local relationships, and does not derive a universal equation that can be used everywhere.

ACKNOWLEDGEMENTS

We wish to thank our colleagues at the CREWES Project and at Hampson-Russell Software for their support and ideas, as well as the sponsors of the CREWES Project.

REFERENCES

- Castagna, J. P., Batzle, M. L., and Eastwood, R. L., 1985, Relationships between compressional-wave and shear-wave velocities in clastic silicate rocks: *Geophysics*, **50**, 571-581.
- Dufour, J., Squires, J., Goodway, W.N., Edmunds, A., and Shook, I., 2002, Integrated geological and geophysical interpretation case study, and Lamé rock parameter extractions using AVO analysis on the Blackfoot 3C-3D seismic data, southern Alberta, Canada: *Geophysics*, **67**, 27-37.
- Hampson, D., Schuelke, J.S., and Quirein, J.A., 2001, Use of multiattribute transforms to predict log properties from seismic data: *Geophysics*, **66**, 220-231.